Age- and brain region-associated alterations of cerebral blood flow in early Alzheimer's disease assessed in AβPP^{SWE}/PS1$^{\Delta E9}$ transgenic mice using arterial spin labeling

YAPEI GUO[1*], XUEYUAN LI[2*], MIN ZHANG[1], NINGNING CHEN[1], SHITAO WU[1], JIANFENG LEI[3], ZHANJING WANG[3], RENZHI WANG[4], JIANPING WANG[1] and HENGFANG LIU[1]

[1]Department of Neurology, The Fifth Hospital of Zhengzhou University; [2]Department of Neurosurgery, The First Hospital of Zhengzhou University, Zhengzhou, Henan 450052; [3]Center for Medical Experiments and Testing, Capital Medical University, Beijing 100069; [4]Department of Neurosurgery, Peking Union Medical College Hospital, Beijing 100052, P.R. China

Received January 4, 2018; Accepted February 6, 2019

DOI: 10.3892/mmr.2019.9950

Abstract. It has been suggested that cerebral blood flow (CBF) alterations may be involved in the pathogenesis of Alzheimer's disease (AD). However, how CBF changes with age has not been detailed in AD, particularly in its early stages. The objective of the present study was to evaluate CBF in four brain regions (the hippocampus, entorhinal cortex, frontoparietal cortex and thalamus) of mice in four age groups, to mimic the respective stages of AD in humans [2 months (pre-clinical), 3.5 months (sub-clinical), 5 months (early-clinical) and 8 months (mid-clinical)], to understand the age-associated changes in selected brain regions and to elucidate the underlying vascular mechanisms. CBF was measured using magnetic resonance imaging-arterial spin labelling (ASL) under identical conditions across the age groups of AβPP^{SWE}/PS1$^{\Delta E9}$ (APP/PS1) transgenic mice with AD. The results indicated age- and brain region-associated changes in CBF were associated with early AD. More precisely, an age-dependent increase in CBF (in the pre- and sub-clinical AD groups) was observed in the frontoparietal cortex and thalamus. Conversely, increased CBF demonstrated an age-dependent decline (in the early- and mid-clinical AD groups) in all examined brain regions. Among the regions, the thalamus had the greatest increase in CBF in the 2 and 3.5 months age groups, which was substantially different compared with the age-matched controls. An extension of vessel area was also noted to be age- and brain region-dependent. In particular, correlation analysis revealed significant associations of CBF with vessel area in the frontoparietal cortex and thalamus of APP/PS1 mice at ages 2 and 3.5 months, indicating that CBF increase may arise from vessel extension. The results of the present study suggested that ASL can detect age- and brain region-associated changes in CBF in mice with AD, and that ASL-measured CBF increase may be a potential diagnostic biomarker for early AD. The observation that CBF increase resulted from vessel extension may aid in the understanding of the vascular role in age-associated development of AD pathology, and provide preclinical evidence for AD patient management.

Correspondence to: Professor HengFang Liu, Department of Neurology, The Fifth Hospital of Zhengzhou University, 3 Kangfu Street, Erqi, Zhengzhou, Henan 450052, P.R. China
E-mail: liuhf1965@163.com

*Contributed equally

Key words: Alzheimer's disease, APP/PS1 mice, arterial spin labeling, cerebral blood flow changes, early diagnosis, biomarker, vessel extension

Introduction

Alzheimer's disease (AD) is the most frequently occurring type of adult dementia with 46.0 million diagnosed individuals globally, causing a loss of one billion dollars to the healthcare industry each year (1). Clinically, patients with AD often present with progressive cognitive decline. Pathologically, AD is characterized by the accumulation of β amyloid (Aβ) peptides in plaques and neuronal loss in a range of brain regions (1,2). Despite this understanding of AD, there are currently no effective measures for treating AD, and the prognosis remains poor (2). Thus, further investigation into the pathogenesis of AD is required for therapeutic exploitation.

Emerging evidence has revealed that cerebral blood flow (CBF) alterations are involved in AD pathogenesis. Clinical studies have demonstrated that CBF disturbance occurs in at-risk elderly subjects, even prior to Aβ accumulation (3-5). Mouse models implicate capillary disturbances as precursors for AD-associated neurodegenerative changes (6). Disturbed CBF may cause a decline in brain perfusion, breakdown of the brain-blood barrier and cerebral clearance disorder, which consequently results in Aβ accumulation (7,8). However, the pattern of AD-associated CBF alterations and how these contribute to AD pathology remains unclear.

Magnetic resonance imaging (MRI)-arterial spin labeling (ASL) provides an *in vivo* technique for measuring CBF by

magnetically labeling arterial water as an endogenous tracer (9). Studies using ASL in humans indicate that brain perfusion changes are already present prior to the onset of AD symptoms (9,10). ASL-measured CBF has been demonstrated to distinguish adults with probable AD from cognitively normal individuals (11). Furthermore, CBF may sensitively predict cognitive decline and conversion to moderate cognitive impairment or AD over time (4). Thus, ASL imaging may serve as a promising tool for the measurement of CBF in preclinical AD.

The hippocampus and entorhinal cortex are thought to be the first regions affected in AD pathology (12). With the progression of AD, an increasing number of regions, including the frontal cortex, are affected (13). Numerous studies have attempted to disclose the factors causing the heterogeneous development of AD pathology (14,15), but few have focused on the contribution of CBF alterations. Advances in micro-MRI techniques have allowed the quantification of CBF in small animals with ASL (9,12), providing novel avenues to study CBF in AD. Detailed study of ASL in AD animals may help to further elucidate AD pathology and identify novel therapeutic strategies.

The aim of the present study was to determine the CBF alterations in four mouse brain regions (the entorhinal cortex, hippocampus, frontoparietal cortex and thalamus). Mice of four varying age groups mimicking the respective stages of AD in humans [2 months (pre-clinical AD), 3.5 months (sub-clinical AD), 5 months (early-clinical AD) and 8 months (mid-clinical AD)] were used to evaluate the age-associated changes in regional CBF in a transgenic mouse model of AD (16), and to subsequently investigate the underlying vascular pathogenesis. The ultimate goal was to identify experimental cues for the detection of AD in patients using ASL.

Materials and methods

Animals. The present study was ethically approved by the Institutional Animal Care and Use Committee of the Medical College of Zhengzhou University (Zhengzhou, China). The use of animals was based on the guidelines published in the National Institutes of Health Guide for the care and use of laboratory animals (16).

$A\beta PP^{SWE}/PS1^{\Delta E9}$ (APP/PS1) transgenic mice (C57BL/6J) evidently exhibit the pathological and behavioral changes of AD and are widely used to mimic human AD in research (17). All mice were tested using polymerase chain reaction-genotyping of the tail tissue to assess their genotype (16). In the present study, a total of 36 female APP/PS1 mice (age, 45-50 days; weight, 15.1-18.2 g) and 36 age-matched female wild-type (WT) littermates (age, 45-50 days; weight, 14.9-18.5 g) were purchased from The Institute of Experimental Animals of The Chinese Academy of Medical Science (Beijing, China). The mice were randomly assigned to four groups. Due to a similar evolution in pathology and behavior with human AD, each group of mice was tested at ages 2, 3.5, 5 or 8 months old (mo) to mimic the pre-, sub-, early- and mid-clinical stage of AD, respectively (APP/PS1 mice, n=9 in each group; WT mice, n=9 in each group) (18). All mice had free access to food and water and were housed in cages in an environmentally controlled room (temperature, 22±1˚C; relative humidity, 40-60%) under a 12-h light/dark cycle.

Morris water maze (MWM) test. The spatial memory learning and memory was assessed using MWM test as previously described (16,19). The test was performed in a white circular pool (diameter, 100 cm) divided into four equal quadrants. The pool was filled with water made opaque with non-fat milk at a temperature of 22±1˚C. Mice were allowed to swim for 60 sec in the pool with a visible platform. Subsequently, an escape platform (diameter, 6 cm) was placed in the center of quadrant II, 1 cm below the water surface. Each mouse performed the test three times per day for 60 sec for 5 successive days, and in each test the mice were allowed to swim freely and to reach the escape platform. The swimming time (escape latency) was recorded and the average time was calculated. At day 6 each mouse performed a test without escape platform and the mouse was allowed to swim freely for 1 min. The number of platform crossings was recorded for each mouse.

MRI-ASL. All MR scans were conducted on a 7.0-T MRI scanner (V.70/16; PharmaScan; Bruker Corporation, Ettlingen, Germany) with a 16 cm bore size and a high-performance gradient system. The signal was received using a 23 mm surface coil. Mice were anesthetized by inhalation of 5% isoflurane, placed in a prone position on the bed, and maintained under anesthesia with 2% isoflurane. The animal's head was secured with a bite bar and two ear bars. Body temperature was maintained at 37˚C with a warm waterbed. The respiratory and heart rates were continuously monitored using a vital sign monitoring system. Anatomical T2-weighted MR images containing the whole brain were acquired on 37 slices at thicknesses of 0.7-mm without any gap between them, with the relaxation enhancement (RARE) sequence with the following parameters: RARE factor 8, repletion time (TE) = 4000 msec, echo time (TR) = 24 msec, field of interest (FOV) = 20 mm x 20 mm, and matrix = 256x256. The T2-weighted images were used to align the subsequent ASL location. ASL images were produced using the Flow-sensitive Alternating Inversion Recovery technique (20,21). A coronal slice at a thickness of 2 mm that simultaneously crossed the frontal lobe and hippocampus was examined. Selective and non-selective ASL images were alternatively acquired. The ASL parameters were as follows: TR = 5000.0 msec; TE = 16.0 msec; FOV = 1.80 cm; slice thickness = 2 mm; matrix = 64x64; number of excitations = 1. The total scan time was ~20 min and 18 sec.

ASL data analysis. The obtained ASL images were analyzed using the workstation software ParaVision 6.0 (Bruker Corporation) to generate CBF images. To determine CBF values, four regions of interest (ROIs) were manually drawn on the non-selective inversion image (Fig. 1), according to the mouse brain atlas by Paxinos and Watson (22). Anatomical T2-weighted images with the same slice location were displayed concurrently for reference. The ROIs were outlined carefully to include the hippocampus, entorhinal cortex, frontoparietal cortex and thalamus, with the involvement of major arteries excluded. The ROIs were then overlaid onto the CBF map with an accurate boundary alignment. From the CBF map, the mean blood flow within the ROIs of each brain was calculated. Bilateral ROIs from the same mouse were analyzed together.

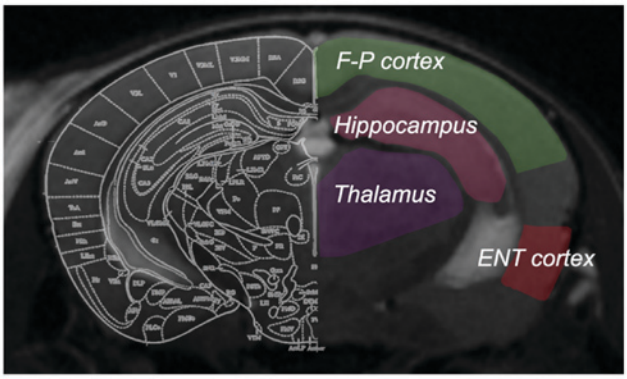

Figure 1. Four regions of interest were examined in the present study, which were outlined on coronal T2-magnetic resonance images of each mouse brain. F-P cortex, frontoparietal cortex; ENT, entorhinal cortex.

Histological evaluation. Subsequent to MR examination, for histological evaluation, the mice were subject to cardiac perfusion with 4% paraformaldehyde at 4˚C for >30 min while remaining deeply anesthetized. Then, brains were collected, post-fixed at room temperature for at least 24 h and sliced into 2-mm-thick coronal blocks. The location of the examined brain blocks was selected based on the distance from the bregma upon ASL imaging. The brain blocks that involved the frontoparietal cortex and dorsal hippocampus were embedded in paraffin and sliced into 6-μm-thick sections for staining.

Immunohistochemical (IHC) staining was used to reveal vascular histology, which was performed as described previously (23). Brain sections were dewaxed, dehydrated, and incubated in epitope retrieval solution (OriGene Technologies, Inc., Beijing, China) at 100˚C for 40 min. Endogenous peroxidase activity was blocked in 4% H_2O_2 at room temperature for 30 min, followed by three washes with PBS. Then, sections were stained with a cluster of differentiation 31 (CD31) antibody (1:500; clone 1A10; cat. no. PA0250; Novocastra; Leica Microsystems, Ltd., Milton Keynes, UK) at 4˚C overnight, followed by incubation with a secondary antibody (1:50; horseradish peroxidase-labeled anti-mouse immunoglobulin G; Invitrogen; Thermo Fisher Scientific, Inc., Waltham, MA, USA) at 37˚C for 60 min and 3,3'-diaminobenzidine (Beijing Zhongshang Jinqiao Biotechnology Co., Ltd., Beijing, China). Counterstaining was performed using hematoxylin (at 100 mg/ml for 30 sec), and then sections were cover-slipped subsequent to dehydration with a graded alcohol series. The obtained sections were captured with a camera (TCS SP2 laser confocal microscope; Leica Microsystems, Ltd., Heidelberg, Germany; magnification, x200) and analyzed using the ImageJ software (version 1.50b; National Institutes of Health, Bethesda, MD, USA). The vessel density (vessel number per mm^2), vessel size (area per vessel) and vessel area (vessel area per mm^2) were calculated based on the CD31-stained sections. Data from bilateral asymmetric brain regions were pooled together for analysis.

Statistical analysis. All results were expressed as the mean ± standard error of the mean. Statistical analyses were performed using GraphPad Prism 6.0 (GraphPad Software, Inc., La Jolla, CA, USA). A two-way analysis of variance (ANOVA) was used to analyze the MWM and ASL data; one-way ANOVA was used to analyze the IHC data, followed by Tukey's multiple comparison tests to assess between-group differences. Pearson's correlation test was used to assess the association between ASL data and vessel area. $P<0.05$ was considered to indicate a statistically significant difference.

Results

Age-associated alterations of regional CBF occur in APP/PS1 mice. In the present study, ASL was used to reveal CBF changes in APP/PS1 mice of varying ages; representative CBF images are presented in Fig. 2A. Compared with WT controls, APP/PS1 mice had increased CBF in the frontoparietal cortex and thalamus at age 2 mo; this increase was more notable at age 3.5 mo. By contrast, CBF was only slightly increased in the entorhinal cortex and hippocampus of APP/PS1 mice at 2 and 3.5 mo compared with WT controls (Fig. 2B). In APP/PS1 mice at 5 mo, increased CBF was reversed in the frontoparietal cortex and thalamus but maintained a consistent level in the entorhinal cortex and hippocampus. At age 8 mo, CBF was reduced in a number of brain regions of APP/PS1 mice even in the WT controls (Fig. 2A). However, MR images revealed no notable structural changes in the brain of APP/PS1 mice at any age (data not shown).

ASL images were quantitatively analyzed based on the ROIs in Fig. 1 (Fig. 2B). Compared with the age-matched WT controls, CBF values in the frontoparietal cortex and thalamus of APP/PS1 mice were significantly increased at 2 mo; this CBF increase was more evident at 3.5 mo, but appeared to decline at 5 mo and returned to basal levels at 8 mo. Despite a slight CBF increase in the hippocampus and entorhinal cortex of APP/PS1 mice at ages 2 and 3.5 mo, increased CBF was not statistically significant at any age including 5 and 8 mo, compared with the age-matched controls. Regional analysis revealed that the frontoparietal cortex and thalamus exhibited transient CBF increases in early AD, whereas the entorhinal cortex and hippocampus exhibited no notable changes in CBF.

Vessel histology. CD31 staining was used to investigate the vascular causes underlying CBF changes; representative images are presented in Fig. 3. Compared with the age-matched WT controls, the vessel size and vessel area were significantly increased in the frontoparietal cortex (Fig. 4A) and thalamus (Fig. 4B) of APP/PS1 mice at 2 and 3.5 mo, with the strongest increase at 3.5 mo. Although APP/PS1 mice also demonstrated an increase in vessel size in the hippocampus (Fig. 4C) and entorhinal cortex (Fig. 4D), the increased size was not significantly larger compared with that of control mice. In APP/PS1 mice at 5 and 8 mo, the vessel size and vessel area in the frontoparietal cortex and thalamus returned to levels equal to that of the control mice, but the vessel size and vessel area vessel decreased in the thalamus and cortex in APP/PS1 mice compared with the age-matched controls. No difference in vessel density was observed in all four ROIs between the APP/PS1 and control mice at any age.

Correlation between ASL data and vessel histology. To investigate potential vascular involvement in CBF alterations, correlation analysis was performed between ASL data and vascular histology. Significant correlations were identified

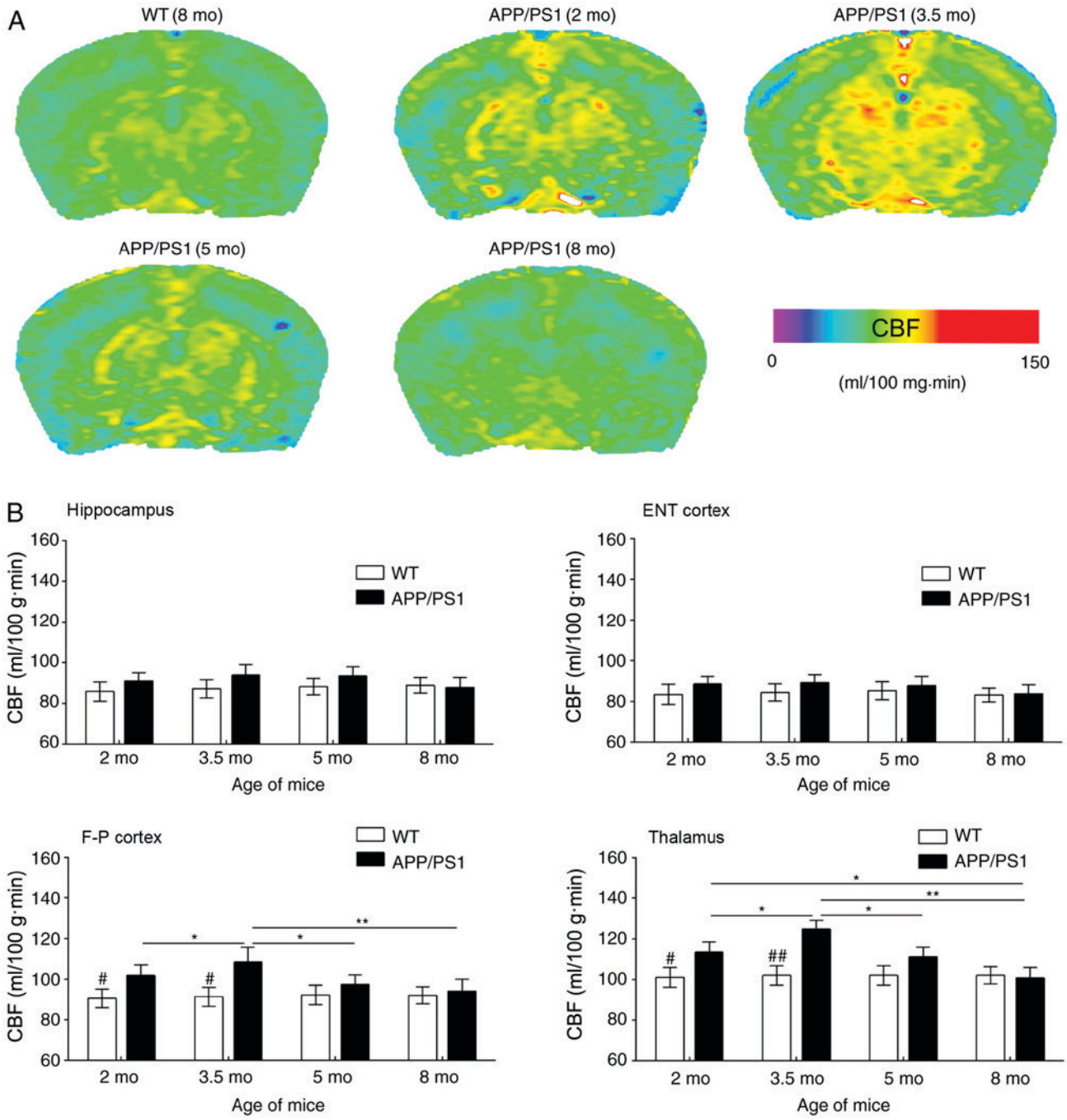

Figure 2. Results of the ASL examination. (A) Typical CBF maps, taken at the frontoparietal lobe and hippocampus from WT (8 mo) and APP/PS1 mice (2, 3.5, 5 and 8 mo). A color map was applied. (B) Age-associated changes in CBF in the ENT cortex, hippocampus, F-P cortex and thalamus for WT and APP/PS1 mice of varying ages. $^{\#}$P<0.05 and $^{\#\#}$P<0.01 vs. age-matched mice; *P<0.05 and **P<0.01 vs. APP/PS1 mice of other age groups. ASL, arterial spin labeling; CBF, cerebral blood flow; WT, wild-type; mo, months old; ENT, entorhinal; F-P, frontoparietal.

between ASL values and vessel area in the frontoparietal cortex and thalamus of APP/PS1 mice at 2 and 3.5 mo, the results of which are summarized in Fig. 5. Results revealed that CBF in the frontoparietal cortex was significantly correlated with vessel area in mice aged 2 (R^2=0.44; P<0.001) and 3.5 mo (R^2=0.42; P<0.001). Further significant correlations were identified between thalamic CBF and vessel area in mice aged 2 (R^2=0.61; P<0.05) and 3.5 mo (R^2=0.67; P<0.001). However, no significant correlations were observed between the CBF and vessel area in mice at 5 and 8 mo. No significant correlations were identified between CBF and vessel density and vessel size in the entorhinal cortex and thalamus in mice of any age (data not shown). These results suggest that regional CBF increase may be associated with vessel extension rather than proliferation.

Discussion

To investigate the role of CBF changes in AD pathogenesis, the present study examined the age- and brain region-associated alterations in CBF in APP/PS1 transgenic mice of varying ages using ASL. A significant increase in CBF in the fronto-parietal cortex and thalamus of APP/PS1 mice was observed

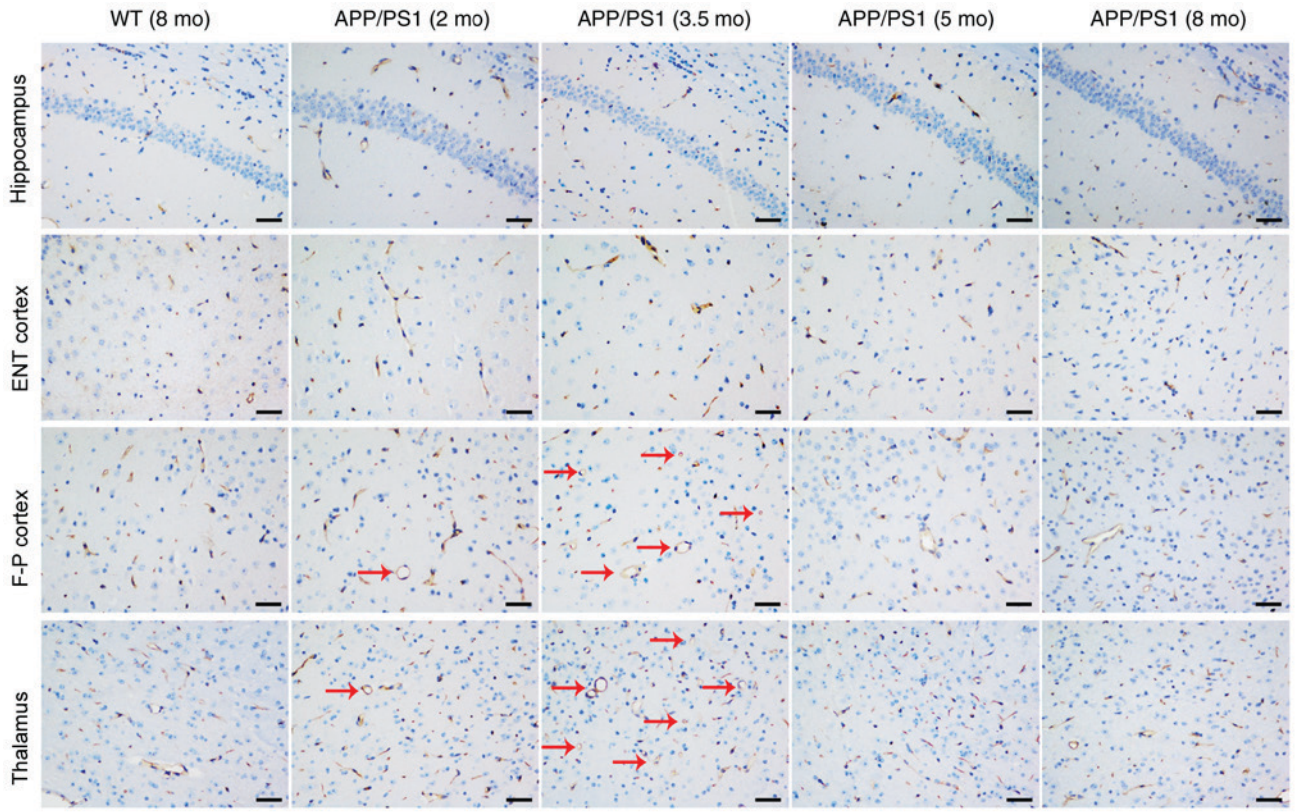

Figure 3. Representative cluster of differentiation 31 staining images of the hippocampus, ENT cortex, F-P cortex and thalamus from WT (8 mo) and APP/PS1 mice (2, 3.5, 5 and 8 mo). Vessels appeared extended (as indicated by the red arrows) in the F-P cortex and thalamus of APP/PS1 mice at ages 2 and 3.5 mo, but not at 5 and 8 mo. No other abnormalities were observed in all brain regions of APP/PS1 mice at any age. Scale bar, 50 μm. WT, wild-type; mo, months old; ENT, entorhinal; F-P, frontoparietal.

prior to cognitive decline, which was then decreased following cognitive decline. By contrast, no notable CBF changes were observed in the entorhinal cortex and hippocampus of APP/PS1 mice. By comparing the CBF in the frontoparietal cortex and thalamus, APP/PS1 mice were distinguished from the controls prior to cognitive decline. In addition, the vessel area, but not vessel density, was notably increased in the frontoparietal cortex and thalamus of APP/PS1 mice, and was significantly correlated with CBF increases in these regions. To the best of our knowledge, the present study is the first to detail the longitudinal changes of regional CBF in early AD in addition to the underlying mechanisms.

Although CBF disorder has been suggested to be involved in AD pathogenesis several times (6,7), the pattern of CBF changes in AD remain unclear, particularly for those with early-stage AD. As AD often has a lengthy period of disease progression (>10 years) prior to the onset of clinical signs (24), the majority of patients are already in the mid- to late-stage of AD when consenting to MRI examination. Thus, it is difficult to observe early CBF changes in patients with AD (24). Model animals provide valuable tools for investigating CBF changes in early AD (25). The present study revealed that APP/PS1 mice exhibited Aβ accumulation but no behavioral impairments at age 2 mo, exhibited regional plaque formation and partial cognitive deficits at 3.5 mo, complete Alzheimer's behaviors and pathology at 5 mo and progressive cognitive decline at age 8 mo, which corresponds with the pre-, sub-, early- and mid-clinical stages of AD, respectively (16). Thus, APP/PS1 mice are ideal subjects for assessing CBF changes associated with early AD.

ASL is a recently-developed technique for determining CBF changes in a non-invasive manner (9). Advances in scanner resolution have allowed for the measurement of regional CBF changes in mice brains using micro-MRI (26,27). In the present study, a ROI-based ASL analysis was performed to assess the age-associated changes of CBF in APP/PS1 mice of varying ages. A significantly higher CBF was observed in the frontoparietal cortex and thalamus of APP/PS1 mice at age 2 mo (prior to cognitive decline) compared with the controls, suggesting that ASL imaging may sensitively reveal CBF changes in early AD. The CBF increase tended to be more prominent at 3.5 mo, but was reduced at 5 and 8 mo. By comparing the CBF at 2 mo, it was demonstrated that APP/PS1 mice were notably different to the controls, suggesting that an ASL-measured CBF increase may be an early biomarker for AD diagnosis. These results are consistent with earlier studies using ASL in humans, demonstrating that CBF changes are present several years prior to the onset of clinical AD symptoms (3). Furthermore, ASL-measured CBF has been revealed to be able to distinguish between cognitively normal individuals, adults at risk for AD and individuals diagnosed with AD (4).

Vascular pathology has been suggested to be involved in AD pathogenesis, which may involve impairment in the structure and function of cerebral blood vessels (28). Accumulating evidence indicates a synergistic association between vascular dysfunction and the accumulation of Aβ and neurofibrillary tangles (28,29).

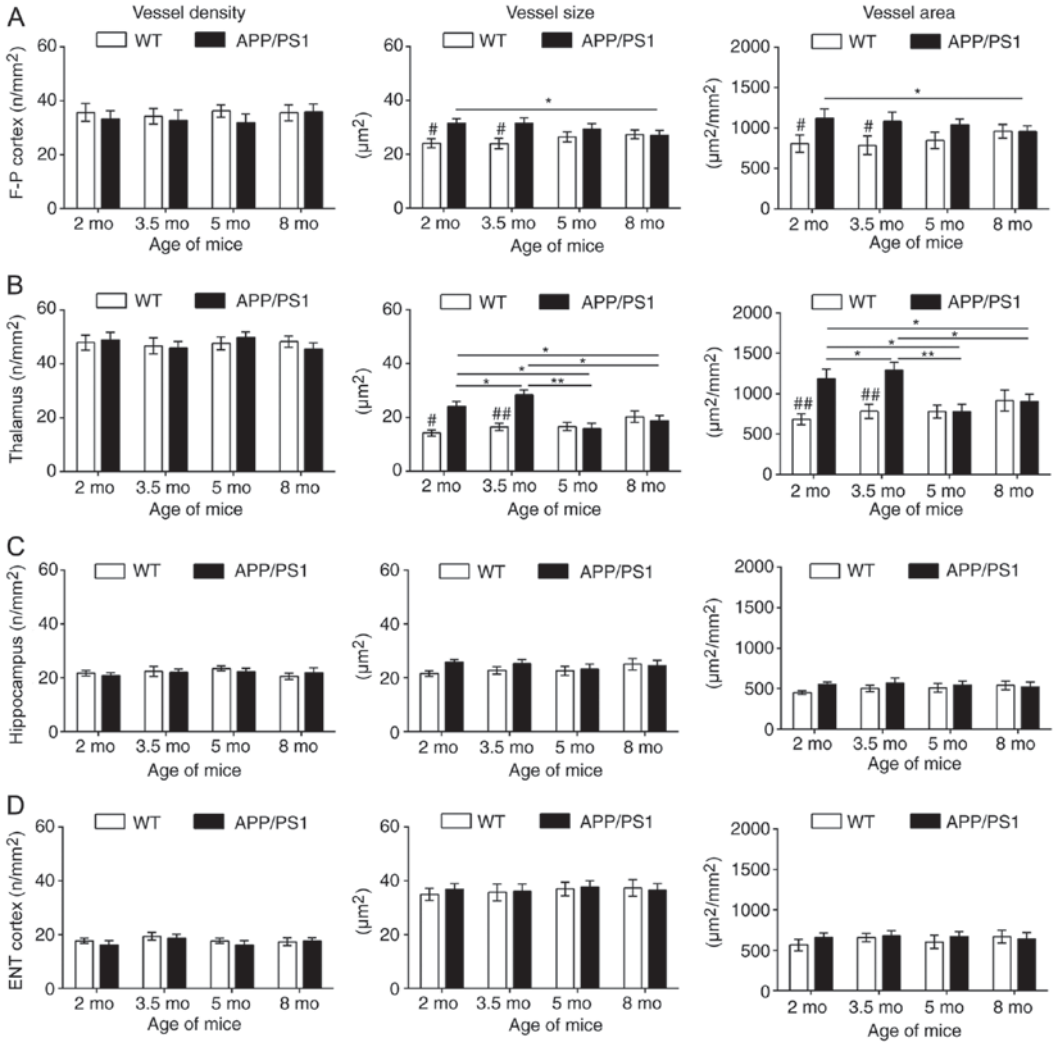

Figure 4. Quantitative analysis of cluster of differentiation 31-staining. Age-associated changes in the vessel density, size and area (per mm^2) in the (A) F-P cortex, (B) thalamus (C) hippocampus and (D) ENT cortex for WT and APP/PS1 mice at age 2, 3.5, 5 and 8 mo. $^{\#}$P<0.05 and $^{\#\#}$P<0.01 vs. age-matched mice; *P<0.05 and **P<0.01 vs. APP/PS1 mice of other age groups. WT, wild-type; mo, months old; ENT, entorhinal; F-P, frontoparietal.

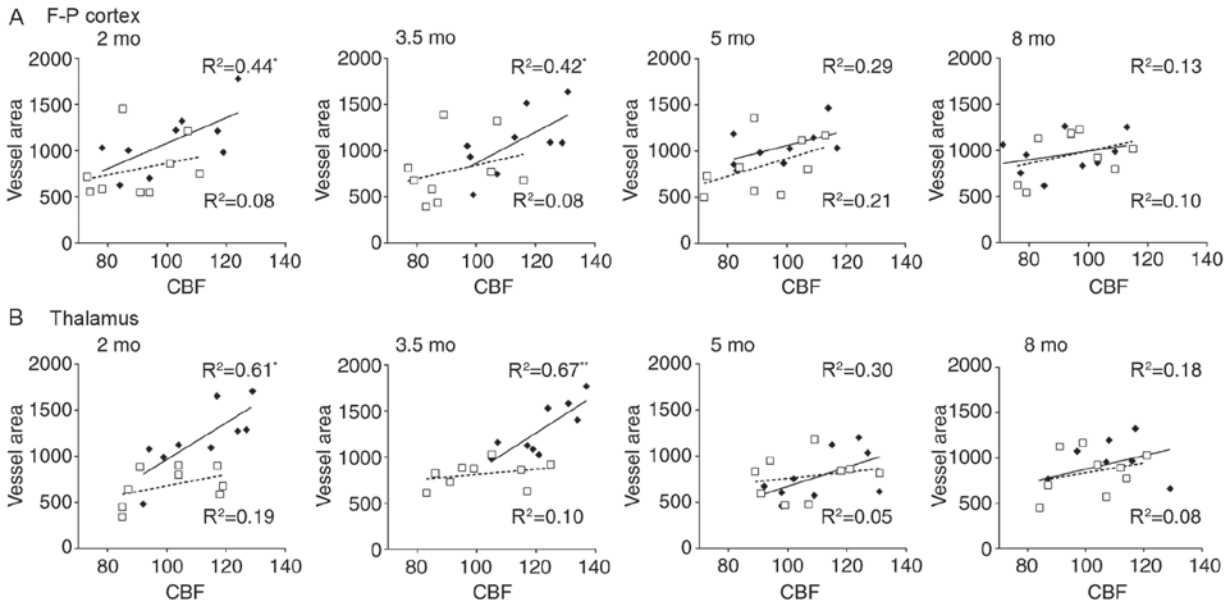

Figure 5. Correlations between regional CBF and vessel histology. Notable associations were observed between CBF values and vessel area in the (A) F-P cortex and (B) thalamus in APP/PS1 mice aged 2 and 3.5 mo, but not 5 and 8 mo. CBF units, ml/100 g·min; Vessel area unit: $\mu m^2/mm^2$. *P<0.05 and **P<0.01. CBF, cerebral blood flow; F-P, frontoparietal; mo, months old.

However, poor cerebral perfusion results in Aβ accumulation and neurofibrillary tangles, and the neurotoxic effects of Aβ in turn impair vascular function, including endothelial function and neurovascular coupling, which consequently causes brain hypoperfusion (28,30,31). In the present study, an extensive reduction of CBF and accumulation of Aβs in the brains of APP/PS1 mice at ages 5 and 8 mo was revealed, supporting the hypothesis of the synergy of vascular dysfunction with Aβ pathology. Despite these results, the cause-effect association between cerebral perfusion and Aβ pathology, particularly in terms of which was first initiated, remains unclear. Encouragingly, regional CBF increases and intracellular Aβ staining but no cognitive decline and visible Aβ plaques in APP/PS1 mice at 2 mo were observed in the present study, suggesting that CBF changes may be initiated subsequent to Aβ overproduction, but precede Aβ plaque formation. Such a result provides the pathological evidence for CBF alterations as an early biomarker for AD, even prior to Aβ plaque formation.

However, CBF increases were heterogeneously distributed in the AD brain. In APP/PS1 mice at 2 and 3.5 mo, increased CBF in the frontoparietal cortex and thalamus, but not in the entorhinal cortex and hippocampus, was observed. The absence of CBF increase in the entorhinal cortex and hippocampus may indicate that these regions are relatively hypoperfused. Furthermore, the higher glucose metabolism that occurs prior to cognitive decline may further exacerbate the hypoperfusion in the hippocampus and entorhinal cortex of APP/PS1 mice, which causes the regions to be vulnerable to Aβ accumulation (32). By contrast, increased CBF in the frontoparietal cortex and thalamus may provide a greater energy supply to enhance regional neuronal activity and Aβ product clearance, thereby delaying Aβ accumulation in plaques (30,33). However, CBF increase was only present for a very short period in the current study, followed by an immediate reduction in CBF. These results were consistent with early reports, and provide basic evidence suggesting that early high brain perfusion occurs prior to cognitive decline in AD (34). The regional heterogeneity of CBF changes, as were revealed in the present study, may be associated with the complicated distribution of AD pathology; but relevant evidence is lacking and requires further investigation.

In addition, the histological basis underlying the alterations in CBF was investigated. The results revealed that increased CBF was associated with a greater vessel area, but not vessel density, in the thalamus and frontoparietal cortex of APP/PS1 mice aged 2 and 3.5 mo, suggesting that vessel extension rather than proliferation results in a CBF increase. This result was supported by the histological analysis, which revealed no increase in vessel density in any brain regions of the APP/PS1 mice. However, no correlations were observed between the changes in CBF and vascular staining in the entorhinal cortex and hippocampus of AD mice, indicative of regionally-absent vessel extension, which may be associated with the vulnerability to AD pathology in these two regions.

There were a number of limitations to the present study. First, the present study does not use one cohort of mice to examine age-associated CBF changes, which may cause within-animal variations. Thus, animal selection and testing time were strictly controlled. Despite this, within-subject changes cannot be avoided, which should be considered when extrapolating the results. Next, the ASL technique has relatively low spatial resolution, low sensitivity to white matter CBF and limited brain coverage. Thus, a brain atlas-guided T2-weighed image was used to outline ROIs, and only larger-sized ROIs majorly involving gray matter were used to enhance sensitivity of ASL. Third, there is a limited specificity of ASL-measured CBF, and it is difficult to distinguish AD pathology from other dementia types, since reduced CBF has been reported in vascular dementia (34). Finally, ASL provides promise but it has not been routinely used in clinical practice. For example, certain methodological issues, including the lack of standardization for ASL in multi-center studies, limit its widespread use. Therefore, the results of the present study represent a conservative revelation of CBF abnormalities occurring in early AD.

In summary, the present study suggests that regional CBF disorder transiently occurs in the brains of APP/PS1 mice with early AD, that a CBF increase in the frontoparietal cortex and thalamus may be an early biomarker for AD diagnosis and that fewer brain vessel extensions in the hippocampus and entorhinal cortex may be associated with their vulnerability to AD pathology. The present study provided evidence that early CBF changes were involved in AD pathology and ASL may be a promising tool for measuring brain perfusion in early AD. However, future research is required to examine whether or to what extent the results may be applied to patients with AD.

Acknowledgements

Not applicable.

Funding

The present study was supported by The National High Technology Research and Development Program of China (grant nos. 2014CB541603 and 2013AA020106) and The National Natural Science Foundation of China (grant nos. 815711137 and 81771247).

Availability of data and materials

The datasets used and/or analyzed during the current study are available from the corresponding author on reasonable request.

Authors' contributions

YG and HL designed the study. YG, XL, NC, SW, JL and ZW performed the experiments and collected data. MZ, RW and JW analyzed and interpreted the data. XL and HL wrote the manuscript. YG, XL and HL revised the manuscript. All authors read and approved the final manuscript.

Ethics approval and consent to participate

The present study was ethically approved by The Institutional Animal Care and Use Committee of The Medical College of Zhengzhou University (Zhengzhou, China).

Patient consent for publication

Not applicable.

Competing interests

The authors declare that they have no competing interests.

References

1. Prince M, Wimo A, Guerchet M, Ali GC, Wu YT and Prina M: An analysis of prevalence, incidence, cost and trends. In: World Alzheimer Report 2015. The Global Impact of Dementia. Alzheimer's Disease International (ADI), London, 2015. https://www.alz.co.uk/research/WorldAlzheimerReport2015.pdf.
2. Li XY, Bao XJ and Wang RZ: Potential of neural stem cell-based therapies for Alzheimer's disease. J Neurosci Res 93: 1313-1324, 2015.
3. Beason-Held LL, Goh JO, An Y, Kraut MA, O'Brien RJ, Ferrucci L and Resnick SM: Changes in brain function occur years before the onset of cognitive impairment. J Neurosci 33: 18008-18014, 2013.
4. Chao LL, Buckley ST, Kornak J, Schuff N, Madison C, Yaffe K, Miller BL, Kramer JH and Weiner MW: ASL perfusion MRI predicts cognitive decline and conversion from MCI to dementia. Alzheimer Dis Assoc Disord 24: 19-27, 2010.
5. Kim SM, Kim MJ, Rhee HY, Ryu CW, Kim EJ, Petersen ET and Jahng GH: Regional cerebral perfusion in patients with Alzheimer's disease and mild cognitive impairment: Effect of APOE Epsilon4 allele. Neuroradiology 55: 25-34, 2013.
6. Nicolakakis N and Hamel E: Neurovascular function in Alzheimer's disease patients and experimental models. J Cereb Blood Flow Metab 31: 1354-1370, 2011.
7. Bell RD and Zlokovic BV: Neurovascular mechanisms and blood-brain barrier disorder in Alzheimer's disease. Acta Neuropathol 118: 103-113, 2009.
8. Zlokovic BV: Role of the brain vascular system and blood-brain barrier transport in clearance of alzheimer's amyloid-beta peptide from the central nervous system. US Patent 20,050,239,062. Filed May 23, 2001; issued October 27, 2005.
9. Inoue Y, Tanaka Y, Hata H and Hara T: Arterial spin-labeling evaluation of cerebrovascular reactivity to acetazolamide in healthy subjects. AJNR Am J Neuroradiol 35: 1111-1116, 2014.
10. Verclytte S, Lopes R, Lenfant P, Rollin A, Semah F, Leclerc X, Pasquier F and Delmaire C: Cerebral hypoperfusion and hypometabolism detected by arterial spin labeling MRI and FDG-PET in early-onset Alzheimer's disease. J Neuroimaging 26: 207-212, 2016.
11. Maier FC, Wehrl HF, Schmid AM, Mannheim JG, Wiehr S, Lerdkrai C, Calaminus C, Stahlschmidt A, Ye L, Burnet M, *et al*: Longitudinal PET-MRI reveals β-amyloid deposition and rCBF dynamics and connects vascular amyloidosis to quantitative loss of perfusion. Nat Med 20: 1485-1492, 2014.
12. Wang Z: Characterizing early Alzheimer's disease and disease progression using hippocampal volume and arterial spin labeling perfusion MRI. J Alzheimers Dis 42 (Suppl 4): S495-S502, 2014.
13. Kerbler GM, Fripp J, Rowe CC, Villemagne VL, Salvado O, Rose S and Coulson EJ; Alzheimer's Disease Neuroimaging Initiative: Basal forebrain atrophy correlates with amyloid β burden in Alzheimer's disease. Neuroimage Clin 7: 105-113, 2014.
14. Badea A, Johnson GA and Jankowsky JL: Remote sites of structural atrophy predict later amyloid formation in a mouse model of Alzheimer's disease. Neuroimage 50: 416-427, 2010.
15. Burns JM, Donnelly JE, Anderson HS, Mayo MS, Spencer-Gardner L, Thomas G, Cronk BB, Haddad Z, Klima D, Hansen D and Brooks WM: Peripheral insulin and brain structure in early Alzheimer disease. Neurology 69: 1094-1104, 2007.
16. Li XY, Men WW, Zhu H, Lei JF, Zuo FX, Wang ZJ, Zhu ZH, Bao XJ and Wang RZ: Age- and brain region-specific changes of glucose metabolic disorder, learning, and memory dysfunction in early Alzheimer's disease assessed in APP/PS1 transgenic mice using ^{18}F-FDG-PET. Int J Mol Sci 17: E1707, 2016.
17. Wang H, Liu J, Zong Y, Xu Y, Deng W, Zhu H, Liu Y, Ma C, Huang L, Zhang L and Qin C: miR-106b aberrantly expressed in a double transgenic mouse model for Alzheimer's disease targets TGF-β type II receptor. Brain Res 1357: 166-174, 2010.
18. Zong YY, Wang XY, Wang HL, Liu YL, Huang L, Ma CM, Zhang LF and Qin C: Continuous analysis of senile plaque and behaviour in APPswe/PSΔE9 double-transgenic gene mouse model of Alzheimer disease. Chin J Comp Med, 2008. http://en.cnki.com.cn/Article_en/CJFDTOTAL-ZGDX200809003.htm.
19. Li X, Zhu H, Sun X, Zuo F, Lei J, Wang Z, Bao X and Wang R: Human neural stem cell transplantation rescues cognitive defects in APP/PS1 model of Alzheimer's disease by enhancing neuronal connectivity and metabolic activity. Front Aging Neurosci 8: 282, 2016.
20. Nasrallah FA, Lee EL and Chuang KH: Optimization of flow-sensitive alternating inversion recovery (FAIR) for perfusion functional MRI of rodent brain. NMR Biomed 25: 1209-1216, 2012.
21. Bitner BR, Brink DC, Mathew LC, Pautler RG and Robertson CS: Impact of arginase II on CBF in experimental cortical impact injury in mice using MRI. J Cereb Blood Flow Metab 30: 1105-1109, 2010.
22. Paxinos G and Franklin KBJ: The Mouse Brain in Stereotaxic Coordinates. Second edition. Academic Press, San Diego, 2001.
23. Zhang L, Liu C, Wu J, Tao JJ, Sui XL, Yao ZG, Xu YF, Huang L, Zhu H, Sheng SL and Qin C: Tubastatin A/ACY-1215 improves cognition in Alzheimer's disease transgenic mice. J Alzheimers Dis 41: 1193-1205, 2014.
24. Hampel H, Prvulovic D, Teipel S, Jessen F, Luckhaus C, Frölich L, Riepe MW, Dodel R, Leyhe T, Bertram L, *et al*: The future of Alzheimer's disease: The next 10 years. Prog Neurobiol 95: 718-728, 2011.
25. Li X, Bao X and Wang R: Experimental models of Alzheimer's disease for deciphering the pathogenesis and therapeutic screening (Review). Int J Mol Med 37: 271-283, 2016.
26. Abrahamson EE, Foley LM, Dekosky ST, Hitchens TK, Ho C, Kochanek PM and Ikonomovic MD: Cerebral blood flow changes after brain injury in human amyloid-beta knock-in mice. J Cereb Blood Flow Metab 33: 826-833, 2013.
27. Hébert F, Grand'maison M, Ho MK, Lerch JP, Hamel E and Bedell BJ: Cortical atrophy and hypoperfusion in a transgenic mouse model of Alzheimer's disease. Neurobiol Aging 34: 1644-1652, 2013.
28. Dickstein DL, Walsh J, Brautigam H, Stockton SD Jr, Gandy S and Hof PR: Role of vascular risk factors and vascular dysfunction in Alzheimer's disease. Mt Sinai J Med 77: 82-102, 2010.
29. Beach TG, Wilson JR, Sue LI, Newell A, Poston M, Cisneros R, Pandya Y, Esh C, Connor DJ, Sabbagh M, *et al*: Circle of Willis atherosclerosis: Association with Alzheimer's disease, neuritic plaques and neurofibrillary tangles. Acta Neuropathol 113: 13-21, 2007.
30. Mattsson N, Tosun D, Insel PS, Simonson A, Jack CR Jr, Beckett LA, Donohue M, Jagust W, Schuff N and Weiner MW; Alzheimer's Disease Neuroimaging Initiative: Association of brain amyloid-β with cerebral perfusion and structure in Alzheimer's disease and mild cognitive impairment. Brain 137: 1550-1561, 2014.
31. Platt B, Welch A and Riedel G: FDG-PET imaging, EEG and sleep phenotypes as translational biomarkers for research in Alzheimer's disease. Biochem Soc Trans 39: 874-880, 2011.
32. Jupp B, Williams J, Binns D, Hicks RJ, Cardamone L, Jones N, Rees S and O'Brien TJ: Hypometabolism precedes limbic atrophy and spontaneous recurrent seizures in a rat model of TLE. Epilepsia 53: 1233-1244, 2012.
33. Michels L, Warnock G, Buck A, Macauda G, Leh SE, Kaelin AM, Riese F, Meyer R, O'Gorman R, Hock C, *et al*: Arterial spin labeling imaging reveals widespread and Aβ-independent reductions in cerebral blood flow in elderly apolipoprotein epsilon-4 carriers. J Cereb Blood Flow Metab 36: 581-595, 2016.
34. Wierenga CE, Hays CC and Zlatar ZZ: Cerebral blood flow measured by arterial spin labeling MRI as a preclinical marker of Alzheimer's disease. J Alzheimers Dis 42 (Suppl 4): S411-S419, 2014.